

Effects of GeO_2 on chlorophyll fluorescence and antioxidant enzymes in apple leaves under strong light

Z.B. WANG*, Y.F. WANG*, J.J. ZHAO*, L. MA*, Y.J. WANG*, X. ZHANG*, Y.T. NIE*, Y.P. GUO***+,
L.X. MEI, and Z.Y. ZHAO*,***

College of Horticulture, Northwest A&F University, Yangling, Shaanxi, China*

Key Laboratory of Horticulture Plant Biology and Germplasm Innovation in Northwest China,

Ministry of Agriculture, Northwest A&F University, Yangling, Shaanxi, China**

Shaanxi Engineering Research Center for Apple, Yangling, Shaanxi, China***

Abstract

In this study, we chose apple leaf as plant material and studied effects of GeO_2 on operation of photosynthetic apparatus and antioxidant enzyme activities under strong light. When exogenous GeO_2 concentration was below 5.0 mg L⁻¹, maximum photochemical quantum yield of PSII and actual quantum yield of PSII photochemistry increased significantly compared with the control under irradiances of 800 and 1,600 $\mu\text{mol}(\text{photon}) \text{m}^{-2} \text{s}^{-1}$. Photosynthetic electron transport chain capacity between Q_A – Q_B , Q_A –PSI acceptor, and Q_B –PSI acceptor showed a trend of rising up with 1.0, 2.0, and 5.0 mg(GeO_2) L⁻¹ and declining with 10.0 mg(GeO_2) L⁻¹. On the other hand, dissipated energy via both ΔpH and xanthophyll cycle decreased remarkably compared with the control when GeO_2 concentration was below 5.0 mg L⁻¹. Our results suggested that low concentrations of GeO_2 could alleviate photoinhibition and 5.0 mg(GeO_2) L⁻¹ was the most effective. In addition, we found, owing to exogenous GeO_2 treatment, that the main form of this element in apple leaves was organic germanium, which means chemical conversion of germanium happened. The organic germanium might be helpful to allay photoinhibition due to its function of scavenging free radicals and lowering accumulation of reactive oxygen species, which was proven by higher antioxidant enzyme activities.

Additional key words: chlorophyll fluorescence; irradiance; photodamage; photosynthetic electron transport chain.

Introduction

Germanium (Ge), a rare element, belongs to the fourth group of the periodic table along with carbon (C), silicon (Si), tin (Sn), and lead (Pb). It exists in the Earth's crust (approximately 1.6 mg kg⁻¹) and has dual nature of metal and nonmetal. Ge can be divided into general inorganic compounds including elemental germanium, GeO_2 , and organic compounds including Ge-132, spiro-germanium

and proxi-germanium (Adams and Thomas 1994, Kaplan *et al.* 2004). Among various kinds of Ge, organic Ge has been confirmed to possess therapeutic attributes including fighting cancer and improving the immune system in human and animals and it was further concluded that the change was attributed to raising radical scavenging activity (Goodman 1988, Tang *et al.* 1997, Yang and Kim 1999).

Received 6 April 2016, accepted 19 June 2017, published as online-first 12 April 2018.

*Corresponding author; e-mail: ypguo@nwsuaf.edu.cn

Abbreviations: ABS – absorption flux; ABS/RC – absorption flux per reaction center of PSII; ABS/CS₀ – absorption flux per sample cross section; APX – ascorbate peroxidase; CAT – catalase; CS – phenomenological energy fluxes per excited cross section; DHAR – dehydroascorbate reductase; DI₀/CS₀ – dissipated energy flux per sample cross section; DI₀/RC – dissipated energy flux per reaction center of PSII; DM – dry mass; FM – fresh mass; F_M – maximal fluorescence; F₀ – initial fluorescence; F_v/F_M – maximum photochemical quantum yield of PSII; F_v/F_{M'} – actual photochemical efficiency; F_s – steady-state fluorescence; GPX – guaiacol peroxidase; GR – glutathione reductase; MDHAR – monodehydroascorbate reductase; NPQ – nonphotochemical quenching coefficient; OJIP – fast chlorophyll fluorescence transients; PETC – photosynthetic electron transport chain; POD – peroxidase; qp – photochemical quenching coefficient; RC – specific energy fluxes per active PSII reaction center; ROS – reactive oxygen species; SOD – superoxide dismutase; TR₀/CS₀ – flux of energy trapping per sample cross-section; TR₀/RC – flux of energy trapping per reaction center of PSII; V_I – relative variable fluorescence at the I-step; V_J – relative variable fluorescence at the J-step; Φ_{NO} – quantum yield of non-light-induced nonphotochemical fluorescence quenching; Φ_{NPQ} – quantum yield of light-induced ΔpH and zeaxanthin-dependent; Φ_{PSII} – actual quantum yield of PSII photochemistry.

Acknowledgements: This work was financially supported by the National Key Technology R&D Program (2014BAD16B06) and the project of the China Agriculture Research System (CARS-28).

Ge exists in all biomaterials including plants and animals (Rosenberg 2009, Sparks *et al.* 2011). A few studies have reported the effects of Ge on plant growth and mineral nutrition uptake in barley (Halperin *et al.* 1995), rice (Seo *et al.* 1995), lettuce (Cheong *et al.* 2009), Chinese cabbage (Han *et al.* 2007), and ginseng seedlings (Yu *et al.* 2005). Barley seedlings accumulated Ge in roots and shoots, and the shoots accumulated Ge linearly as an exogenous Ge concentration increased (Halperin *et al.* 1995). In hydroponically-grown lettuce treated with a low concentration of GeO_2 , Ge was taken up by roots and barely moved to shoots. Furthermore, with all types of Ge treatment, plants showed no changes in their phenotype of leaf shape and color, including necrosis or chlorosis (Han *et al.* 2007).

Although several previous studies have reported the toxicity and uptake of Ge in plants and explored the effects of Ge on photosynthesis and antioxidant enzyme systems in leaves (Tarakhovskaya *et al.* 2012, Liu *et al.* 2016), there is still no research on the operation of photosynthetic apparatus. Various studies have demonstrated ROS accumulating more under high light intensity and excess ROS causing photoinhibition (Takahashi and Murata 2008). In biological systems, the antioxidant enzyme system plays an important role in resistance to oxidative stress and is helpful to maintain the normal biological

structure and physiological activities (Apel and Hirt 2004).

Apple, one of the most important fruits in the world, has been confirmed containing Ge in our preliminary study. In consideration of therapeutic attributes of Ge, apple may have the effect of improving antioxidant ability for humans; it indicates the urgency of the study on influences of exogenous Ge on apple trees. In this study, we chose apple leaf as the test material and tried to reveal the effects of GeO_2 on operation of photosynthetic apparatus and antioxidant enzyme system under two different light intensities. Graphite furnace atomic absorption spectrometry was used to investigate the uptake, accumulation, chemical conversion of Ge in apple leaves with exogenous GeO_2 . Furthermore, through modulated chlorophyll (Chl) fluorescence and Chl fluorescence transients (OJIP), more information about the P_{680} , electron transport between P_{680} and P_{700} , and P_{700} (PETC) and partitioning of absorbed light energy *via* photochemistry and thermal dissipation processes can be obtained. Moreover, in order to explain the influence of exogenous GeO_2 on apple photosynthetic apparatus, we determined activities of seven antioxidant enzymes and contents of hydrogen peroxide (H_2O_2) and superoxide anion (O_2^\cdot) in order to explain how exogenous GeO_2 influences apple photosynthetic apparatus.

Materials and methods

Plant material and growth conditions: Potted three-year-old dwarf apple (*Malus domestica* Borkh. cv. Red Fuji)/M26 (*Malus pumila* Mill.) trees were selected as test material. The experiments were conducted at Northwest A&F University, Yangling City (34°20'N, 108°24'E), Shaanxi Province, China. All plants were grown in plastic pots (height of 38 cm, diameter of 23 cm) filled with a mixed soil (volume ratio of field topsoil to organic matter was 2:1, pH 7.5, relative soil water content of 75%). Prior to the start of our trials, all trees were well watered and regulated daily to avoid water deficiency, diseases, and insect pests.

Treatments: In order to ensure GeO_2 entry into apple leaves, the marked mature leaves were cut at the petiole and immediately dipped into water solution containing 0, 1.0, 2.0, 5.0, and 10.0 mg(GeO_2) L^{-1} , respectively, and maintained at 25°C under irradiance of 20 $\mu\text{mol}(\text{photon}) \text{m}^{-2} \text{s}^{-1}$ for 24 h. Subsequently, the leaves in each treatment were divided into two parts and exposed under two light intensities of 800 and 1,600 $\mu\text{mol}(\text{photon}) \text{m}^{-2} \text{s}^{-1}$ for 4 h before the determination of the parameters.

Chl content in apple leaves: Fresh leaves (0.1 g) were ground in 80% acetone to extract both Chl *a* and Chl *b*. The samples were kept in the dark for 24 h at 4°C, and the extracts were centrifuged for 2 min at 3000 rpm and then analyzed by a spectrophotometer (UV-2800, Unic, Shanghai, China). The absorbance readings were per-

formed at 665 nm for Chl *a*, at 649 nm for Chl *b*. Pigment quantities were calculated according to Lichtenthaler *et al.* (1987).

Ge content: The content of organic and inorganic Ge in apple leaves was determined using graphite furnace atomic absorption spectrometry, as described by McMahon *et al.* (2004). Plant samples were cleaned with distilled water, then oven-dried at 70°C for 72 h and ground to a fine powder with a mortar. The powder with particle size below 100 mm were collected for analysis. Powder (0.1 g) from each blade was fully carbonated and then was transformed into muffle furnace to be ashed at 600°C for 4 h. Through this process, all forms of Ge in apple leaf converted into elemental Ge and its content can be determined as the total Ge content using graphite furnace atomic absorption spectrometry. Then free inorganic Ge in apple leaf could be obtained from another 0.1 g of leaf powder through water bath (100°C) and its content can be determined using graphite furnace atomic absorption spectrometry. The content of organic Ge in each blade can be calculated by the difference between the content of total Ge and the content of inorganic Ge.

Modulated Chl fluorescence parameters were measured at room temperature of 25°C with a pulse amplitude modulation fluorometer (PAM-2500, Walz, Germany) after leaves were dark-adapted for 20 min. The fluorometer was connected to a trifurcated fiber-optic (2010-F) and to

a computer with data acquisition software (*PAM Win 3.02*). The experimental protocol was basically followed according to Genty *et al.* (1989).

The minimum fluorescence (F_0) and maximum fluorescence (F_M) were determined, respectively, using measuring light [$<1 \mu\text{mol}(\text{photon}) \text{ m}^{-2} \text{ s}^{-1}$] and a 0.8-s saturating pulse at $6,000 \mu\text{mol}(\text{photon}) \text{ m}^{-2} \text{ s}^{-1}$. Actinic light of $619 \mu\text{mol}(\text{photon}) \text{ m}^{-2} \text{ s}^{-1}$ was used. After about 5 min, the steady-state value of fluorescence (F_S) was thereafter recorded and a second saturating pulse at $6,000 \mu\text{mol}(\text{photon}) \text{ m}^{-2} \text{ s}^{-1}$ was imposed to determine F_M in the light-adapted state (F_M'). F_0' was basal fluorescence after $5 \mu\text{mol}(\text{photon}) \text{ m}^{-2} \text{ s}^{-1}$ of far-red irradiation at $720\text{--}730 \text{ nm}$ for 4 s, which excites PSI and oxidizes the plastoquinone and Q_A pools associated with PSII. With these original parameters above, the maximum photochemical quantum yield of PSII (F_v/F_M), efficiency of excitation capture by PSII (F_v'/F_M'), actual quantum yield of PSII photochemistry (Φ_{PSII}), coefficient of photochemical fluorescence quenching (q_p), coefficient of nonphotochemical fluorescence quenching *via* ΔpH (q_N), coefficient of non-photochemical fluorescence quenching *via* xanthophyll cycle (NPQ), quantum yield of non-light-induced non-photochemical fluorescence quenching (Φ_{NO}), quantum yield of light-induced ΔpH and zeaxanthin-dependent nonphotochemical fluorescence quenching (Φ_{NPO}) were calculated as defined by previous studies (Kitajima and Butler 1975, Schreiber *et al.* 1986, Genty *et al.* 1989, Bilger and Björkman 1990, Kramer *et al.* 2004).

OJIP transients and analysis of relative parameters: The Chl a fluorescence transients (OJIP-test) were also measured at room temperature (25°C) with a pulse amplitude modulation fluorometer (*PAM-2500*, Walz, Germany) after the leaves were dark-adapted for 20 min. Each Chl a fluorescence transient was analyzed according to the JIP-test utilizing original data: (1) the minimum fluorescence intensity [the fluorescence intensity at $20 \mu\text{s}$, F_0]; (2) the maximum fluorescence intensity (F_M); (3) the fluorescence intensity at 2 ms (J-step, F_J) and 30 ms (I-step, F_I) (Streibet and Govindjee 2011).

The relative variable fluorescence intensity at J-step (V_J) and I-step (V_I) were calculated as: $V_t = (F_t - F_0)/(F_M - F_0)$. In JIP-test, $ET_0/TR_0 = 1 - V_J$, reflecting the probability that a PSII trapped electron is transferred from Q_A to Q_B ; $RE_0/TR_0 = 1 - V_I$, reflecting the probability a PSII trapped electron is transferred until PSI acceptors; and $RE_0/ET_0 = (1 - V_I)/(1 - V_J)$, reflecting the probability an electron from Q_B is transferred until PSI acceptors. In addition, in the JIP-test, $F_v/F_M \times ET_0/TR_0$, $F_v/F_M \times RE_0/TR_0$, $F_v/F_M \times RE_0/ET_0$ reflect the quantum yield of the electron transport flux from Q_A to Q_B , quantum yield of the electron transport flux until the PSI electron acceptors, quantum yield of the electron transport flux from Q_B until PSI acceptors, respectively.

The parameters reflecting absorbed photon flux were

calculated as follows: $\text{ABS/RC} = (M_0/V_J) \times [1/(F_v/F_M)]$, quantifying average absorbed photon flux per PSII reaction center (RC); $\text{ABS/CS}_0 = F_0$, quantifying absorbed photon flux per cross section (CS). The parameters that reflect trapped exciton flux were calculated as follows: $\text{TR}_0/\text{RC} = M_0/V_J$, quantifying maximum trapped exciton flux per PSII RC; $\text{TR}_0/\text{CS}_0 = F_v/F_M \times F_0$, quantifying maximum trapped exciton flux per CS. The parameters that reflect energy dissipation were calculated as follows: $\text{DI}_0/\text{RC} = \text{ABS/RC} - \text{TR}_0/\text{RC}$, quantifying dissipated energy flux per active PSII RC; $\text{DI}_0/\text{CS}_0 (t = 20 \mu\text{s}) = \text{ABS/CS}_0 - \text{TR}_0/\text{CS}_0$, quantifying dissipated energy flux per CS.

H_2O_2 and O_2^\cdot contents were determined according to Chen (2013). Fresh leaf powder of 0.1 g was homogenized with 1.8 ml of 5% (w/v) trichloroacetic acid and then centrifuged at $16,000 \times g$ for 10 min. The supernatant was neutralized to pH 7.5 with 17 M NH_4OH , and used for assay immediately.

For O_2^\cdot assay, the extract was divided into two aliquots of 100 μl . Superoxide dismutase [SOD, 50 U, 10,000 U mg^{-1} (protein), Sigma, USA] was added to one aliquot (blank). Both the blank and the other aliquot without SOD were added to 0.9 ml with 50 mM Tris-HCl (pH 7.5), and then kept at room temperature for 10 min, before adding 100 μl of 5 mM 2,3-bis(2-methoxy-4-nitro-5-sulfo-phenyl)-2H-tetrazolium-5-carboxanilide inner salt. The reaction mixture was incubated at room temperature for 10 min, and then the absorbance at 470 nm was monitored. The difference on absorbance between the blank and the other aliquot was used to calculate the concentration of O_2^\cdot using an extinction coefficient of $21.6 \text{ mM}^{-1} \text{ cm}^{-1}$.

For H_2O_2 assay, the extract was divided into two aliquots of 100 μl . Catalase [CAT, 20 U, 20,000 U mg^{-1} (protein), Sigma, USA] was added to one aliquot (blank). Both the blank and the other aliquot without CAT were added to 0.5 ml with 50 mM Tris-HCl (pH 7.5) buffer, and then kept at room temperature for 10 min, following the addition of 0.5 ml of colorimetric reagent. The colorimetric reagent was made daily by mixing 1:1 (v/v) 0.3 mM potassium titanium oxalate and 0.3 mM 4-(2-pyridylazo)resorcinol monosodium salt. The assay mixture was incubated at room temperature for 15 min and then the absorbance at 508 nm was monitored (*UV-2800*, Unic, Shanghai, China). The difference on absorbance between the blank and the other aliquot was used to calculate the concentration of H_2O_2 using an extinction coefficient of $39.4 \text{ mM}^{-1} \text{ cm}^{-1}$.

Antioxidant enzymes activities: Fresh tissue samples (0.1 g each) were homogenized with 1.8 ml of 100 mM phosphate buffer saline PBS (pH 7.0) containing 5% (w/v) polyvinylpyrrolidone, 1.0 mM EDTA and 1% *Triton X-100*. The homogenates were centrifuged at $13,000 \times g$ for 20 min at 4°C and the supernatants were used for enzyme assays. All enzyme activities were calculated on fresh mass basis.

CAT (EC 1.11.1.6) activity was determined by monitoring the decrease in absorbance at 240 nm due to decomposition of H₂O₂ (Díaz-Vivancos *et al.* 2008). The 1.0 ml of reaction mixture contained 50 mM PBS (pH 7.0), 10 mM H₂O₂, and 20 μ l of enzyme extract. This reaction was initiated by adding H₂O₂. One CAT unit was defined as the amount of enzyme necessary to decompose 1 mM(H₂O₂) min⁻¹ under the above-mentioned assay conditions. The specific CAT activity was expressed as U g⁻¹(FM) min⁻¹.

Peroxidase (POD, EC 1.11.1.7) activity was measured by the increase in absorbance at 470 nm due to guaiacol oxidation (Nickel and Cunningham 1969). The reaction mixture of 1.0 ml contained 10 mM guaiacol, 10 mM H₂O₂, and 20 μ l of enzyme extract. The reaction was started by adding H₂O₂. One unit of POD activity was defined as the amount of the enzyme causing a change in absorbance at 470 nm of 0.01 per min. The specific POD activity [U g⁻¹(FM) min⁻¹] = $(\Delta A_{470} \times V) / (M \times V_s \times 0.01 \times t)$, in expressions, ΔA_{470} was the change of A₄₇₀ during every minute; V was total volume of crude enzyme solution; V_s was volume of crude enzyme used in the determination; M was mass of fresh materials; t was reaction time in min.

SOD (EC 1.15.1.1) activity was assayed by monitoring the inhibition of the photochemical reduction of nitroblue tetrazolium (NBT), according to the methods of Rao and Sresty (2000). The 1.0 ml of reaction mixture contained 50 mM PBS (pH 7.8), 6.5 mM methionine, 50 μ M NBT, 10 μ M EDTA, 20 μ M riboflavin, and 20 μ l of enzyme extract. A reaction mixture lacking enzyme served as the control. All mixtures were stirred under darkness in small glass test tubes, and then irradiated for 5 min by fluorescent lamps [160 μ mol(photon) m⁻² s⁻¹] before measured at 560 nm. The mixture that lacked enzyme was used to zero the absorbance at 560 nm (UV-2800, Unic, Shanghai, China). One unit of SOD was defined as the amount of enzyme that produced 50% inhibition of NBT reduction under assay conditions. The specific SOD activity was expressed as U g⁻¹(FM).

Ascorbate peroxidase (APX, EC 1.11.1.11) activity was evaluated by monitoring the decrease in absorbance at 290 nm as ascorbate was oxidized (Nakano and Asada 1981). The 1.0 ml of reaction mixture contained 50 mM PBS (pH 7.6), 0.1 mM EDTA, 0.5 mM reduced ascorbate (AsA), 1 mM H₂O₂, and 20 μ l of enzyme extract. The reaction was initiated by adding H₂O₂. One unit of APX activity was defined as the amount of the enzyme causing a change in 1.0 μ mol AsA was oxidized per min. The specific APX activity [U g⁻¹(FM) min⁻¹] = $(\Delta A_{290} \times V) / (2.8 \times M \times V \times t)$, in expressions, ΔA_{290} was the change of A₂₉₀ during 30 s; V was total volume of crude enzyme solution; 2.8 mM⁻¹ cm⁻¹ was an extinction coefficient; M was mass of fresh materials; t was reaction time, 0.5 min.

Dehydroascorbate reductase (DHAR, EC 1.8.5.1)

activity was determined by monitoring the increase in absorbance at 265 nm due to AsA formation (Nakano and Asada 1981). The 1.0 ml of reaction mixture contained 50 mM potassium phosphate buffer (pH 7.6), 2.5 mM reduced glutathione (GSH), 0.1 mM EDTA, 0.2 mM dehydroascorbate (DHA), and 20 μ l of enzyme extract. The reaction was initiated by adding DHA. One unit of DHAR activity was defined as the amount of the enzyme causing a change in 1.0 μ mol AsA formation per min at absorbance at 265 nm. The specific DHAR activity [U g⁻¹(FM) min⁻¹] = $(\Delta A_{265} \times V) / (M \times V_s \times 5.42 \times t)$, in expressions, ΔA_{265} was the change of A₂₆₅ during every minute; V was total volume of crude enzyme solution; V_s was volume of crude enzyme used in the determination; M was mass of fresh materials; 5.42 mM⁻¹ cm⁻¹ was an extinction coefficient; t was reaction time, 3.0 min.

Monodehydroascorbate reductase (MDHAR, EC 1.6.5.4) activity was assayed by monitoring the decrease in absorbance at 340 nm due to NADH oxidation (Nakano and Asada 1981). The 1.0 ml of reaction mixture contained 50 mM PBS (pH 7.6), 2.5 mM AsA, 0.1 mM EDTA, 0.1 mM NADH, 0.5 units of AsA oxidase (EC 1.10.3.3), and 20 μ l of enzyme extract. The reaction was initiated by adding AsA oxidase. One unit of MDHAR activity was defined as the amount of the enzyme causing a change in 1.0 μ mol NADH oxidation per min. The specific MDHAR activity was expressed as U g⁻¹(FM) min⁻¹.

Glutathione reductase (GR, EC 1.6.4.2) activity was measured by monitoring the decrease in absorbance at 340 nm due to NADPH oxidation (Zhang and Kirkham 1996). The 1.0 ml of reaction mixture contained 50 mM PBS (pH 7.0), 0.2 mM EDTA, 0.1 mM NADPH, 0.25 mM oxidized glutathione (GSSG), and 100 μ l of enzyme extract. The reaction was initiated by adding NADPH. The GR activity was calculated by measuring the change in absorbance at 340 nm for GSSG-dependent oxidation of NAPDH. One unit of GR activity was defined as the amount of the enzyme causing a change in 1.0 μ mol NADPH oxidation per min. The specific GR activity [U g⁻¹(FM) min⁻¹] = $(\Delta A_{340} \times V) / (M \times V_s \times 6.22 \times t)$, in expressions, ΔA_{340} was the change of A₃₄₀ during every minute; V was total volume of crude enzyme solution; V_s was volume of crude enzyme used in the determination; M was mass of fresh materials; 6.22 mM⁻¹ cm⁻¹ was an extinction coefficient; t was reaction time, 3.5 min.

Statistical analysis: All statistical analysis were conducted with the SPSS software (Version 19, SPSS Inc., USA). Analysis of variance (ANOVA) were used to evaluate the effects of treatment. Significant differences between plants with different treatment were calculated at *p*<0.05 level, using *Duncan*'s tests. Values were presented as the means of ten replicates \pm standard error (SE). Figures were finished with the Origin Pro software (Version 7.5, OriginLab Inc., USA).

Results

Ge accumulation: Compared with the control, exogenous GeO_2 application significantly increased endogenous Ge contents of both inorganic and organic germanium form in leaves (Table 1). Specifically, inorganic germanium content in leaves treated with 1.0, 2.0, 5.0, and 10.0 $\text{mg}(\text{GeO}_2) \text{ L}^{-1}$ was 2.6, 11.2, 14.2, and 21.9 times higher than the control, respectively; organic Ge content in leaves was 30.7, 44.8, 61.8, and 102.8 times higher than the control, respectively. Although the exogenous Ge was applied in its inorganic form (GeO_2), in apple leaves, organic Ge content was significantly higher than that of inorganic form.

Change of Chl content in apple leaves: Chl *a* content increased with 1.0, 2.0, and 5.0 $\text{mg}(\text{GeO}_2) \text{ L}^{-1}$ treatment compared with control, but there was no remarkable difference between 10.0 $\text{mg} \text{ L}^{-1}$ and control (Table 2). The total Chl (*a+b*) content changed similarly as Chl *a*. Chl *b* content did not increase as much as Chl *a*, although its content with 5.0 $\text{mg} \text{ L}^{-1}$ was significantly higher than that with 1.0 and 10.0 $\text{mg}(\text{GeO}_2) \text{ L}^{-1}$ treatments and control. For Chl *a/b*, only the value after 10.0 $\text{mg} \text{ L}^{-1}$ treatment was significantly lower than others.

Table 1. Contents of total Ge, inorganic Ge, and organic Ge in apple leaves with treatments of different GeO_2 concentrations. Each value is the mean \pm standard error of ten independent measurements. Means \pm SE ($n = 6$). Different *lowercase letters* indicate significant differences between treatments ($P < 0.05$).

GeO_2 [$\text{mg} \text{ L}^{-1}$]	Total Ge [$\text{mg} \text{ kg}^{-1}(\text{DM})$]	Inorganic Ge [$\text{mg} \text{ kg}^{-1}(\text{DM})$]	Organic Ge [$\text{mg} \text{ kg}^{-1}(\text{DM})$]
0	$1.53 \pm 0.22^{\text{e}*}$	$0.19 \pm 0.06^{\text{d}}$	$1.34 \pm 0.18^{\text{e}}$
1.0	$43.23 \pm 4.14^{\text{d}}$	$0.70 \pm 0.19^{\text{c}}$	$42.53 \pm 3.95^{\text{d}}$
2.0	$63.70 \pm 3.90^{\text{c}}$	$2.32 \pm 0.22^{\text{b}}$	$61.39 \pm 3.99^{\text{c}}$
5.0	$87.06 \pm 16.28^{\text{b}}$	$2.88 \pm 0.75^{\text{b}}$	$84.18 \pm 17.03^{\text{b}}$
10.0	$143.41 \pm 10.18^{\text{a}}$	$4.35 \pm 0.35^{\text{a}}$	$139.06 \pm 10.52^{\text{a}}$

Modulated Chl fluorescence parameters: In apple leaves with 1.0, 2.0 and 5.0 $\text{mg}(\text{GeO}_2) \text{ L}^{-1}$, the Chl fluorescence parameters, such as F_v/F_M , F_v'/F_M' , q_P , q_L , and

Φ_{PSII} , increased significantly under both 800 and 1, 600 $\mu\text{mol}(\text{photon}) \text{ m}^{-2} \text{ s}^{-1}$ (Table 3). These five parameters declined after 10.0 $\text{mg}(\text{GeO}_2) \text{ L}^{-1}$ treatment. On the other hand, the value of NPQ and q_N , both quantifying the energy dissipation, declined in apple leaves with 1.0, 2.0, and 5.0 $\text{mg}(\text{GeO}_2) \text{ L}^{-1}$ and rose at the concentration of 10.0 $\text{mg} \text{ L}^{-1}$. Meanwhile, the change of NPQ and q_N affected the value of Φ_{NPQ} , but not Φ_{NO} . Φ_{NPQ} decreased with 1.0, 2.0, and 5.0 $\text{mg}(\text{GeO}_2) \text{ L}^{-1}$ and increased in 10.0 $\text{mg}(\text{GeO}_2) \text{ L}^{-1}$, while Φ_{NO} was maintained stable compared with control.

OJIP transients and relative parameters: Clearly, in Chl fluorescence transient, exogenous GeO_2 changed the momentary maximum fluorescence intensity of J-step and I-step (Fig. 1). The parameters including $1 - V_J$, $1 - V_I$, $(1 - V_I)/(1 - V_J)$, $F_v/F_M \times (1 - V_J)$, $F_v/F_M \times (1 - V_I)$, and $F_v/F_M \times (1 - V_I)/(1 - V_J)$ all showed a rising trend along with the increase of GeO_2 concentration and reached a peak when it was 5.0 $\text{mg} \text{ L}^{-1}$, then all declined at 10.0 $\text{mg} \text{ L}^{-1}$ (Fig. 2). A significant difference in $1 - V_J$ between 800 and 1,600 $\mu\text{mol}(\text{photon}) \text{ m}^{-2} \text{ s}^{-1}$ was observed as well as in $F_v/F_M \times (1 - V_J)$, while other four parameters with same GeO_2 treatment were almost equal under the two light intensities.

We also determined partitioning of absorbed light energy *via* photochemical reaction and thermal dissipation. The change of parameters including ABS/RC, ABS/CS₀, TR₀/RC, TR₀/CS₀, DI₀/RC, DI₀/CS₀ were shown in Fig. 3. The light absorption per residue active RC (ABS/RC) and per CS (ABS/CS₀) in control and at 10.0 $\text{mg} \text{ L}^{-1}$ were higher than that at 1.0, 2.0, and 5.0 $\text{mg}(\text{GeO}_2) \text{ L}^{-1}$ (Fig. 3A,D). Moreover, the values of ABS/RC and ABS/CS₀ under 1,600 $\mu\text{mol}(\text{photon}) \text{ m}^{-2} \text{ s}^{-1}$ were both lower than that under 800 $\mu\text{mol}(\text{photon}) \text{ m}^{-2} \text{ s}^{-1}$. TR₀/RC and TR₀/CS₀ did not change remarkably with different concentrations of exogenous GeO_2 solutions and different light intensities (Fig. 3B,E). DI₀/RC and DI₀/CS₀, dissipated energy flux per PSII RC and CS, decreased at 1.0, 2.0, and 5.0 $\text{mg}(\text{GeO}_2) \text{ L}^{-1}$ (Fig. 3C,F), meaning lesser dissipation of excess excitation energy in these chloroplasts.

Table 2. Effect of different GeO_2 concentrations on chlorophyll (Chl) content in apple leaves. Means \pm SE ($n = 6$). Different *lowercase letters* indicate significant differences between treatments ($P < 0.05$).

GeO_2 [$\text{mg} \text{ L}^{-1}$]	Chl (<i>a+b</i>) [$\text{mg} \text{ g}^{-1}$]	Chl <i>a</i> [$\text{mg} \text{ g}^{-1}$]	Chl <i>b</i> [$\text{mg} \text{ g}^{-1}$]	Chl <i>a/b</i>
0	$2.21 \pm 0.07^{\text{d}}$	$1.64 \pm 0.05^{\text{d}}$	$0.57 \pm 0.01^{\text{c}}$	$2.85 \pm 0.05^{\text{ab}}$
1.0	$2.38 \pm 0.03^{\text{c}}$	$1.76 \pm 0.03^{\text{c}}$	$0.62 \pm 0.01^{\text{b}}$	$2.86 \pm 0.03^{\text{a}}$
2.0	$2.48 \pm 0.05^{\text{b}}$	$1.84 \pm 0.02^{\text{b}}$	$0.64 \pm 0.02^{\text{ab}}$	$2.87 \pm 0.04^{\text{a}}$
5.0	$2.62 \pm 0.04^{\text{a}}$	$1.94 \pm 0.03^{\text{a}}$	$0.68 \pm 0.02^{\text{a}}$	$2.86 \pm 0.02^{\text{a}}$
10.0	$2.27 \pm 0.03^{\text{d}}$	$1.67 \pm 0.04^{\text{d}}$	$0.60 \pm 0.02^{\text{bc}}$	$2.76 \pm 0.04^{\text{b}}$

Table 3. The effect of different GeO_2 concentrations on modulated chlorophyll fluorescence in apple leaves. Each value is the mean \pm standard error of ten independent measurements. Means \pm SE ($n=6$). Different lowercase letters indicate significant differences between treatments ($P<0.05$).

Treatments		Modulated chlorophyll fluorescence parameters						Φ_{NO}		
Light intensity [$\mu\text{mol}(\text{photon}) \text{ m}^{-2} \text{ s}^{-1}$]	GeO_2 [mg L^{-1}]	F_v/F_M	F_v'/F_M'	q_p	q_L	q_N	Φ_{PSII}	Φ_{NPQ}	Φ_{NO}	
800	0	0.708 \pm 0.004 ^a	0.538 \pm 0.017 ^c	0.590 \pm 0.011 ^c	0.427 \pm 0.012 ^{bc}	0.676 \pm 0.011 ^d	1.120 \pm 0.056 ^d	0.318 \pm 0.018 ^{cd}	0.361 \pm 0.019 ^c	0.322 \pm 0.012 ^a
	1.0	0.746 \pm 0.008 ^b	0.582 \pm 0.010 ^b	0.637 \pm 0.018 ^{ab}	0.443 \pm 0.012 ^b	0.625 \pm 0.018 ^e	0.983 \pm 0.043 ^e	0.371 \pm 0.017 ^b	0.311 \pm 0.018 ^d	0.319 \pm 0.011 ^a
	2.0	0.769 \pm 0.005 ^a	0.606 \pm 0.012 ^a	0.654 \pm 0.013 ^{ab}	0.446 \pm 0.016 ^b	0.611 \pm 0.011 ^c	0.968 \pm 0.048 ^e	0.393 \pm 0.021 ^{ab}	0.298 \pm 0.012 ^d	0.309 \pm 0.011 ^a
	5.0	0.780 \pm 0.006 ^a	0.614 \pm 0.007 ^a	0.665 \pm 0.012 ^a	0.473 \pm 0.010 ^a	0.603 \pm 0.016 ^e	0.933 \pm 0.057 ^e	0.408 \pm 0.014 ^a	0.286 \pm 0.014 ^d	0.306 \pm 0.008 ^a
	10.0	0.710 \pm 0.012 ^c	0.509 \pm 0.015 ^c	0.587 \pm 0.016 ^c	0.467 \pm 0.018 ^{ab}	0.690 \pm 0.011 ^d	1.131 \pm 0.058 ^d	0.295 \pm 0.007 ^d	0.374 \pm 0.013 ^e	0.322 \pm 0.010 ^a
	1,600	0	0.696 \pm 0.008 ^c	0.449 \pm 0.016 ^d	0.574 \pm 0.009 ^c	0.400 \pm 0.010 ^d	0.745 \pm 0.013 ^b	1.423 \pm 0.053 ^{ab}	0.256 \pm 0.010 ^g	0.427 \pm 0.017 ^{ab}
1,600	1.0	0.699 \pm 0.010 ^c	0.463 \pm 0.017 ^d	0.590 \pm 0.016 ^c	0.423 \pm 0.008 ^{bc}	0.744 \pm 0.015 ^b	1.366 \pm 0.042 ^b	0.271 \pm 0.010 ^f	0.419 \pm 0.013 ^{bc}	0.310 \pm 0.010 ^a
	2.0	0.695 \pm 0.010 ^c	0.465 \pm 0.014 ^d	0.598 \pm 0.007 ^c	0.430 \pm 0.016 ^{bc}	0.745 \pm 0.011 ^b	1.365 \pm 0.030 ^b	0.276 \pm 0.011 ^{ef}	0.416 \pm 0.011 ^{bc}	0.308 \pm 0.009 ^a
	5.0	0.695 \pm 0.010 ^c	0.479 \pm 0.015 ^d	0.632 \pm 0.010 ^b	0.434 \pm 0.013 ^{bc}	0.731 \pm 0.014 ^{bc}	1.281 \pm 0.030 ^c	0.300 \pm 0.016 ^e	0.393 \pm 0.010 ^c	0.307 \pm 0.010 ^a
	10.0	0.650 \pm 0.015 ^d	0.402 \pm 0.013 ^e	0.595 \pm 0.014 ^c	0.413 \pm 0.012 ^{cd}	0.771 \pm 0.010 ^a	1.451 \pm 0.041 ^a	0.240 \pm 0.011 ^g	0.447 \pm 0.011 ^a	0.313 \pm 0.011 ^a

H_2O_2 and $\text{O}_2^{\cdot-}$ contents were similarly affected by GeO_2 application in apple leaves (Fig. 4). Under two light conditions, H_2O_2 contents in the leaves significantly decreased with 1.0, 2.0, and 5.0 $\text{mg}(\text{GeO}_2) \text{ L}^{-1}$. For $\text{O}_2^{\cdot-}$, its contents descended with above three concentrated GeO_2 solutions under 1,600 $\mu\text{mol}(\text{photon}) \text{ m}^{-2} \text{ s}^{-1}$, but under 800 $\mu\text{mol}(\text{photon}) \text{ m}^{-2} \text{ s}^{-1}$, it only continually descended significantly with 1.0 and 2.0 $\text{mg}(\text{GeO}_2) \text{ L}^{-1}$ and did not show significant difference between 2.0 and 5.0 $\text{mg}(\text{GeO}_2) \text{ L}^{-1}$. However, the accumulation of H_2O_2 and $\text{O}_2^{\cdot-}$ significantly increased by application of 10.0 $\text{mg}(\text{GeO}_2) \text{ L}^{-1}$. And furthermore, apple leaves generated more H_2O_2 and $\text{O}_2^{\cdot-}$ under 1,600 $\mu\text{mol}(\text{photon}) \text{ m}^{-2} \text{ s}^{-1}$ than that under 800 $\mu\text{mol}(\text{photon}) \text{ m}^{-2} \text{ s}^{-1}$. These results indicate Ge could decrease the accumulation of ROS in the apple leaves and alleviate ROS-induced membrane damage.

Activities of CAT, POD and SOD were enhanced in apple leaves along with the rise of the exogenous GeO_2 concentration and reached a peak at the concentration of 5.0 $\text{mg}(\text{GeO}_2) \text{ L}^{-1}$ and then the activities of these three enzymes declined after the treatment by 10.0 $\text{mg}(\text{GeO}_2) \text{ L}^{-1}$ (Fig. 5). For the two light intensities, 1,600 $\mu\text{mol}(\text{photon}) \text{ m}^{-2} \text{ s}^{-1}$ stimulated the activities of CAT and POD noticeably compared to those under 800 $\mu\text{mol}(\text{photon}) \text{ m}^{-2} \text{ s}^{-1}$. Similar difference was not found for the activity of SOD with GeO_2 application.

Activities of ascorbate–glutathione cycle enzymes: Exogenous GeO_2 application significantly changed the activities of antioxidant enzymes including MDHAR, DHAR, APX, and GR under both light intensities (Fig. 6). Among them, MDHAR and DHAR were influenced by exogenous GeO_2 in a similar way. Activities of the two enzymes increased with the increasing concentration of GeO_2 solution compared with the control and the rising trend slowed down when the concentration was above 5.0 mg L^{-1} . The activities of APX and GR in apple leaves with GeO_2 treatment were enhanced along with the increase of exogenous GeO_2 concentration, but started to decline when the concentration was above 5.0 mg L^{-1} . In addition, activities of four enzymes of MDHAR, DHAR, APX, and GR under 1,600 $\mu\text{mol}(\text{photon}) \text{ m}^{-2} \text{ s}^{-1}$ were higher than that under 800 $\mu\text{mol}(\text{photon}) \text{ m}^{-2} \text{ s}^{-1}$ after GeO_2 treatment.

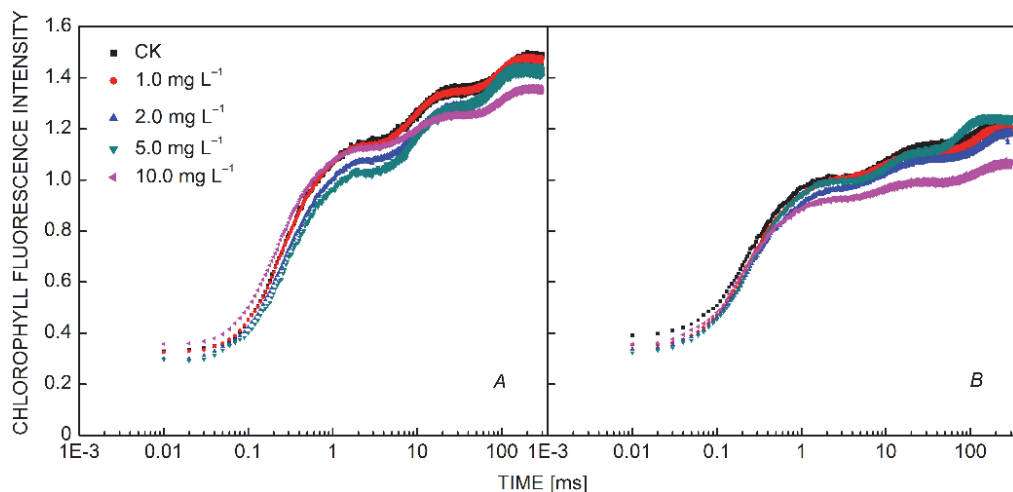


Fig. 1. Effect of different GeO_2 concentrations on chlorophyll fluorescence intensity in JIP-test under $800 \mu\text{mol}(\text{photon}) \text{m}^{-2} \text{s}^{-1}$ (A) and $1,600 \mu\text{mol}(\text{photon}) \text{m}^{-2} \text{s}^{-1}$ (B) in apple leaves.

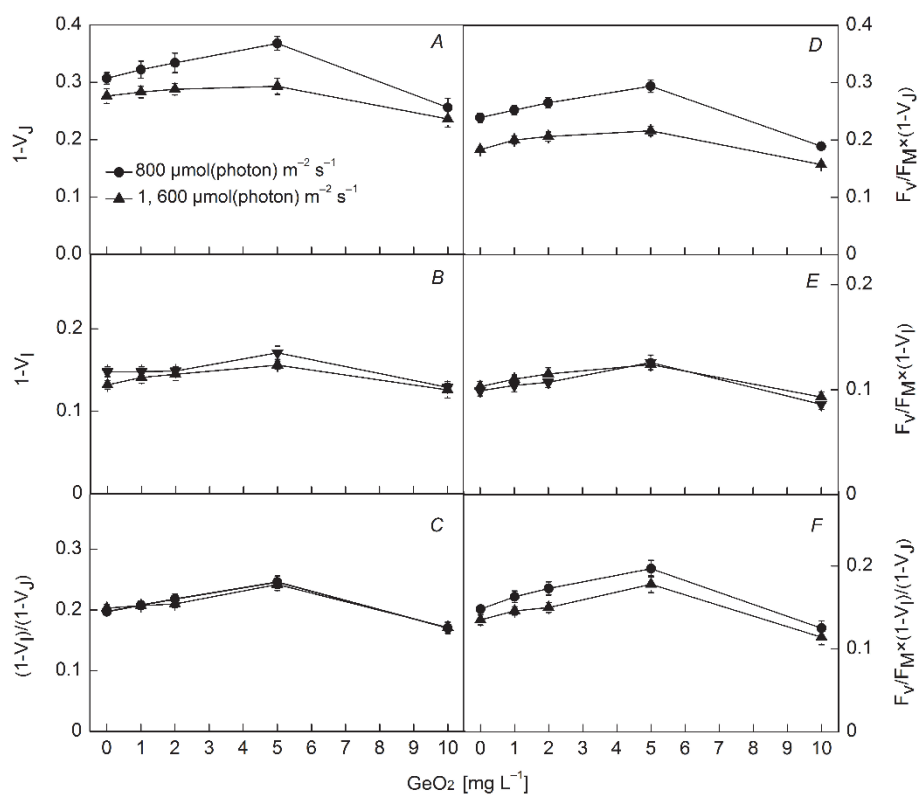


Fig. 2 Change in values of (A) $1 - V_I$, (B) $1 - V_I$, (C) $(1 - V_I)/(1 - V_J)$, (D) $F_v/F_M \times (1 - V_J)$, (E) $F_v/F_M \times (1 - V_I)$, and (F) $F_v/F_M \times (1 - V_I)/(1 - V_J)$ in apple leaves under 800 and $1,600 \mu\text{mol}(\text{photon}) \text{m}^{-2} \text{s}^{-1}$ for 4 h with different GeO_2 concentrations.

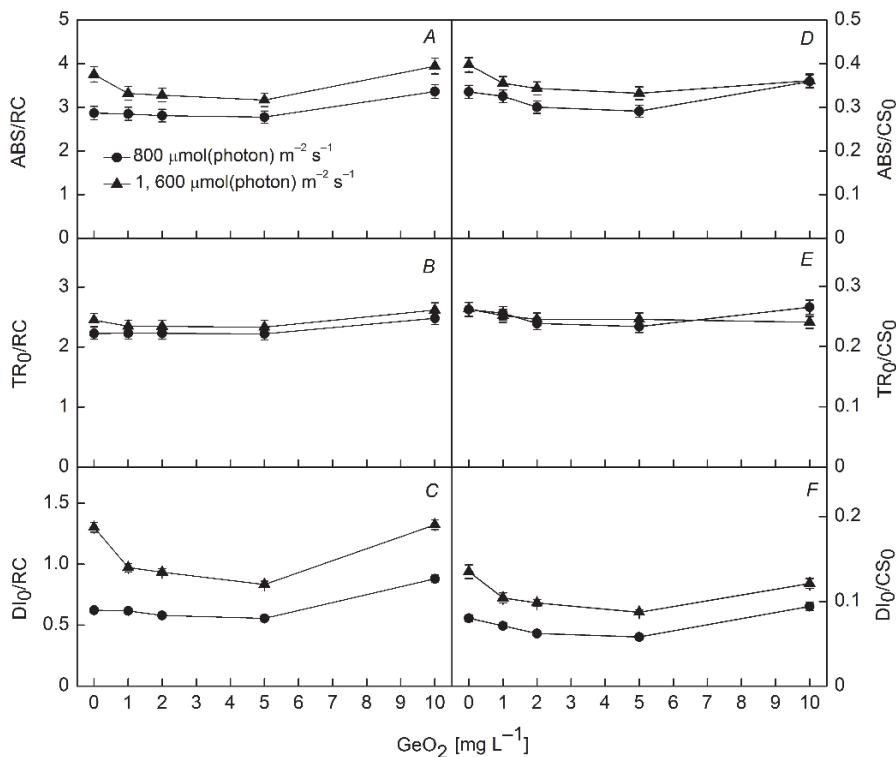


Fig. 3. Change in values of (A) ABS/RC, (B) TR₀/RC, (C) DI₀/RC, (D) ABS/CS₀, (E) TR₀/CS₀, and (F) DI₀/CS₀ in apple leaves under 800 and 1,600 $\mu\text{mol}(\text{photon}) \text{m}^{-2} \text{s}^{-1}$ for 4 h with different GeO₂ concentrations.

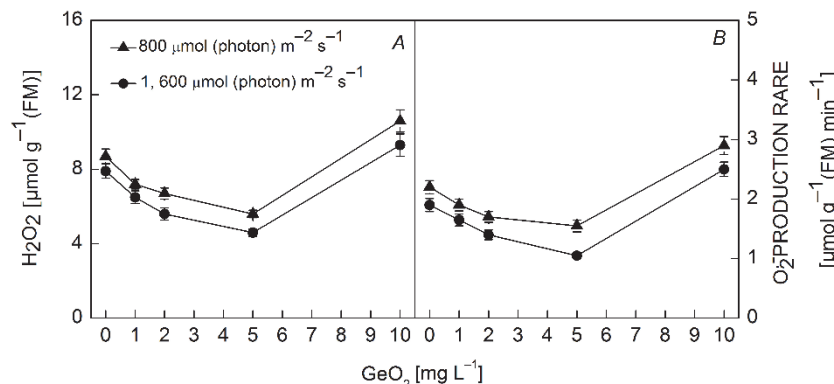


Fig. 4. Effect of different GeO₂ concentrations on ROS content in apple leaves including (A) H₂O₂ content and (B) O₂^{·-} content in apple leaves under 800 and 1,600 $\mu\text{mol}(\text{photon}) \text{m}^{-2} \text{s}^{-1}$ for 4 h.

Discussion

Regarding to the effects of Ge on plants, previous studies focused on the accumulation of Ge in medicinal herb or herbaceous plants and tried to find a critical toxicity value of this element (Halperin *et al.* 1995, Yu *et al.* 2005, Han *et al.* 2007, Lim *et al.* 2008, Cheong *et al.* 2009). Previous studies also found Ge could be helpful to scavenge ROS (Munakata *et al.* 1987), but it remains unclear on how Ge influences photosynthetic apparatus, in which ROS generates under high light and environmental stress. In this study, in order to reveal effects of GeO₂ on photosynthesis

and its mechanism, we monitored the response of apple leaves with different exogenous GeO₂ treatment using Chl fluorescence, concentration or formation rate of ROS and activities of antioxidant enzymes.

Compared with the control, contents of inorganic and organic Ge in leaves treated with exogenous GeO₂ increased significantly. After further analysis, we found that organic Ge content was the main form of Ge in apple leaves, although the exogenously applied Ge was in the inorganic form (GeO₂) (Table 1). It suggests that

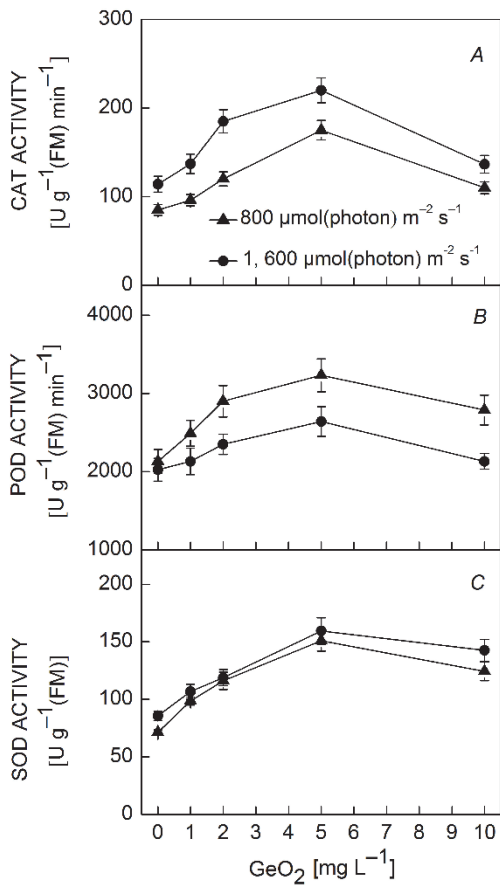


Fig. 5. Effect of different GeO_2 concentrations on (A) CAT activity, (B) POD activity, (C) SOD activity in apple leaves under 800 and 1,600 $\mu\text{mol}(\text{photon}) \text{m}^{-2} \text{s}^{-1}$ for 4 h.

exogenous GeO_2 converted into the organic form after entering into the apple leaves. The results are in accordance with studies in rice (Matsumoto *et al.* 1975).

Therefore, we speculate that the *Malus* has the capacity to change free inorganic form into a bound organic form.

The change of Chl contents implies exogenous GeO_2 had a significant impact on Chl *a* content but not on Chl *b* content (Table 2). As Chl *a* has the most important role among photosynthetic pigments, exogenous GeO_2 may subsequently affect the function of photosynthetic apparatus which can be proved by modulated fluorescence parameters and fast fluorescence transient analysis.

As reported by previous researches, modulated fluorescence parameters could reflect photosynthetic performance including changes in PSII photochemistry efficiency, linear electron flux, and capacity of the Calvin cycle (Meyer *et al.* 2001). F_v/F_M , the maximum photochemical quantum yield of PSII, could provide a simple and rapid way to evaluate the photosynthetic performance (Henriques 2009, Zai *et al.* 2012, Zhang *et al.* 2014). In our study, F_v/F_M of apple leaves with 1.0, 2.0, and 5.0 $\text{mg}(\text{GeO}_2) \text{L}^{-1}$ increased significantly and declined at 10.0 $\text{mg}(\text{GeO}_2) \text{L}^{-1}$ under both 800 and 1,600 $\mu\text{mol}(\text{photon}) \text{m}^{-2} \text{s}^{-1}$ (Table 3). Based on the changes of Φ_{PSII} , q_p , q_L and F_v/F_M' , we suggest GeO_2 in appropriate concentration may facilitate the performance of photosynthetic apparatus. On the other hand, NPQ and q_N , quantifying energy dissipation through xanthophyll cycle and ΔpH (Jahns and Holzwarth 2012), both declined in apple leaves with 1.0, 2.0, and 5.0 $\text{mg}(\text{GeO}_2) \text{L}^{-1}$ and rose with 10.0 $\text{mg}(\text{GeO}_2) \text{L}^{-1}$. Along with the rise of NPQ and q_N , Φ_{NPQ} decreased at 1.0, 2.0 and 5.0 $\text{mg}(\text{GeO}_2) \text{L}^{-1}$ and increased at 10.0 $\text{mg}(\text{GeO}_2) \text{L}^{-1}$, while Φ_{NO} remained at a steady level compared with control (Tab 1). If we consider $\Phi_{\text{NPQ}} + \Phi_{\text{NO}} + \Phi_{\text{PSII}} = 1$, the drop of Φ_{NPQ} with 1.0, 2.0, and 5.0 $\text{mg}(\text{GeO}_2) \text{L}^{-1}$ resulted in the rise of Φ_{PSII} . Opposite response of photochemical capacity and energy dissipation indicates effects of GeO_2 on photosynthetic apparatus.

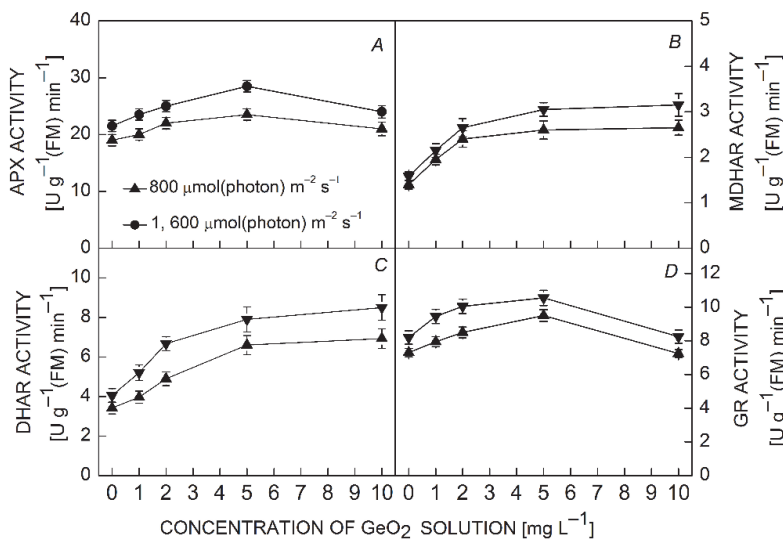


Fig. 6. Effects of different GeO_2 concentrations on ascorbate-glutathione cycle including (A) APX activity, (B) MDHAR activity, (C) DHAR activity, (D) GR activity in apple leaves under 800 and 1,600 $\mu\text{mol}(\text{photon}) \text{m}^{-2} \text{s}^{-1}$ for 4 h.

The fast fluorescence transient analysis is a fast and nondestructive method to measure the response of PSII activity to environmental changes and has been used widely for characterizing the photochemical quantum yield of PSII photochemistry and electron transport activity (Streibet and Govindjee 2011, Schansker *et al.* 2005). In the present study, the JIP-test was also used to assess the photosynthetic performance of apple leaves with different GeO_2 solutions under strong light (Fig. 1). The OJIP curves showed high light-induced decrease in apple leaves (Fig. 1B). This phenomenon was similar to Antarctic lichens under high light stress (Balarinová *et al.* 2014). The momentary maximum fluorescence intensity (J-step and I-step) represents the subsequent kinetic bottlenecks of the electron transport chain (Strasser *et al.* 2000, Lazár 2006). These limitations come from the exchange of a reduced plastoquinone molecule with an oxidized one at Q_B site (J-step), and the reoxidation of plastoquinol (PQH_2 , I-step) (Schansker *et al.* 2005). Such change of Chl fluorescence intensity in O–J, O–I, J–I phase can represent PETC activity between Q_A – Q_B , Q_A –PSI acceptor, Q_B –PSI acceptor, respectively (Wang *et al.* 2012). We found clearly the electron transport from Q_A to Q_B , reflected by $1 - V_J$ and $F_v/F_M \times (1 - V_J)$, was affected more than the electron transport from Q_B to PSI by exogenous GeO_2 and two light intensities (Fig. 2).

In order to elucidate the performance of photosynthetic apparatus in more details, we applied the parameters derived from the Chl a fluorescence transient including ABS/RC, ABS/CS₀, TR₀/RC, TR₀/CS₀, DI₀/RC, DI₀/CS₀, to give a further insight into partitioning of absorbed light energy in apple leaves treated with GeO_2 . ABS/RC and ABS/CS₀, average absorbed photon flux per PSII RC and per CS, both presented a downward trend with 1.0, 2.0, 5.0 $\text{mg}(\text{GeO}_2) \text{ L}^{-1}$, and then rose with 10.0 $\text{mg}(\text{GeO}_2) \text{ L}^{-1}$ (Fig. 3A,D). ABS/RC and ABS/CS₀ can be regarded as a probe to understand the average amount of absorbing antenna chlorophylls per fully active (Q_A -reducing) reaction center, which offers a way to detect eventual inactivation of RCs. In the present study, those two parameters could tell that the number of Q_A -reducing RCs and the density of RCs per CS in control and 10.0 mg L^{-1} group were lower than those at 1.0, 2.0 and 5.0 $\text{mg}(\text{GeO}_2) \text{ L}^{-1}$. Irradiance of 1,600 $\mu\text{mol}(\text{photon}) \text{ m}^{-2} \text{ s}^{-1}$ can more easily inactivate PSII RC than that of 800 $\mu\text{mol}(\text{photon}) \text{ m}^{-2} \text{ s}^{-1}$ therefore under high irradiation, the number of Q_A -reducing RCs were lower in apple leaves. It can explain ABS/RC and ABS/CS₀ under 1,600 $\mu\text{mol}(\text{photon}) \text{ m}^{-2} \text{ s}^{-1}$ were higher than those under 800 $\mu\text{mol}(\text{photon}) \text{ m}^{-2} \text{ s}^{-1}$. TR₀/RC and TR₀/CS₀ (Fig. 3B,E) in our study did not change remarkably with different exogenous GeO_2 solutions and different light intensities. Data of DI₀/RC and DI₀/CS₀ (Fig. 3C,F) showed that dissipated energy per PSII RC and CS dropped significantly, This also suggests that high irradiation declines photoprotection capacity. Apparently, GeO_2 application in range of values of 1.0–5.0 mg L^{-1} resulting in apple leaves absorbing less light

energy and dissipating more energy per PSII RC and CS, which reduced the damage of strong light to photosynthetic apparatus. However, it also did not exclude the possibility for downregulation of photosynthetic excitation pressure (Li *et al.* 2015).

As the site of photosynthesis, chloroplasts are also the major source of ROS such as $\text{O}_2^{\cdot-}$ and H_2O_2 . ROS can be generated by the direct transfer of the excitation energy from Chl to produce singlet oxygen or by oxygen reduction in the Mehler reaction in the chloroplasts, leading to membrane lipid peroxidation (Stepien and Klobus 2005, Gill and Tuteja 2010). In our study, we observed apple leaves treated with 1.0, 2.0, and 5.0 $\text{mg}(\text{GeO}_2) \text{ L}^{-1}$ accumulated less $\text{O}_2^{\cdot-}$ and H_2O_2 (Fig. 4), which could be responsible for the increase of photosynthetic performance.

During evolution, a series of antioxidant enzymes are developed to scavenge ROS in plants. Concisely, SOD plays a central role in the enzymatic defense system in removing $\text{O}_2^{\cdot-}$ (Diao *et al.* 2014) and CAT has a potential to directly dismutate H_2O_2 into H_2O and O_2 , which is indispensable for ROS-detoxification (Garg and Manchanda 2009, Hasanuzzaman and Fujita 2011). So to figure out the reason for the decreased contents of ROS, we determined the activities of antioxidant enzymes. In our study, with low concentration of GeO_2 treatment, CAT, SOD and POD activities increased, especially the activities of CAT and POD were noticeably higher under high light intensity (Fig. 5). Apart from CAT, POD and SOD, it is well known that the ascorbate-glutathione cycle is the key mechanism to scavenge ROS in plant chloroplasts and its higher efficiency under abiotic and biotic stress is responsible for the alleviation of oxidant damage to chloroplasts (Nakano and Asada 1981). In this cycle, APX plays the most important role in removing H_2O_2 . MDHAR, DHAR, and GR are mainly responsible for providing substrates for APX through the formation of reduced AsA and GSH. Our results showed that exogenous GeO_2 below 5.0 mg L^{-1} promoted the activities of APX, MDHAR, DHAR and GR (Fig. 6). Such response of antioxidant defense system may be a protecting mechanism for apple leaves through improving the activity to clear excess ROS under strong light.

In this study, we investigated effects of GeO_2 on photosynthetic performance of apple leaves under strong light. With the application of GeO_2 , the photosynthetic performance of apple leaves including maximum photochemical quantum yield of PSII, the actual photochemical quantum yield of PSII and photochemical quenching efficiency at 1.0, 2.0, and 5.0 $\text{mg}(\text{GeO}_2) \text{ L}^{-1}$ remarkably increased under both light intensities. In the meantime, dissipated energy through xanthophyll cycle and ΔpH decreased noticeably compared with the control when the GeO_2 concentration was below 5.0 mg L^{-1} . Also, PETC capacity was also found to be impacted by exogenous GeO_2 among Q_A – Q_B , Q_A –PSI acceptor, and Q_B –PSI acceptor, PETC happened in Q_A to Q_B was affected the most showing a rising trend with low concentration of GeO_2 treatment. The decrease in ROS accumulation and

increase of antioxidant enzymatic defense system might be the reason for the drop of dissipated energy and the promotion of photosynthetic performance in apple leaves treated with GeO_2 solution below 5.0 mg L^{-1} . As organic

Ge has been reported to have a function scavenging free radicals, such response of antioxidant ability under strong light could be related to the transformation of Ge chemical form, from exogenous inorganic GeO_2 to organic Ge.

Reference

Adams J.H., Thomas D.: Germanium and germanium compounds. – In: Kirk-Othmer (ed.): Encyclopedia of Chemical Technology. Pp. 540-555. Wiley, New York 1994.

Apel K., Hirt H.: Reactive oxygen species: metabolism, oxidative stress, and signal transduction. – *Annu. Rev. Plant Biol.* **55**: 373-399, 2004.

Balarinová K., Barták M., Hazdrová J. *et al.*: Changes in photosynthesis, pigment composition and glutathione contents in two Antarctic lichens during a light stress and recovery. – *Photosynthetica* **52**: 538-547, 2014.

Bilger W., Björkman O.: Role of the xanthophyll cycle in photoprotection elucidated by measurements of light-induced absorbance changes, fluorescence and photosynthesis in leaves of *Hedera canariensis*. – *Photosynth. Res.* **25**: 173-185, 1990.

Chen C., Li H., Zhang D. *et al.*: The role of anthocyanin in photoprotection and its relationship with the xanthophyll cycle and the antioxidant system in apple peel depends on the light conditions. – *Physiol. Plantarum* **149**: 354-366, 2013.

Cheong Y.H., Kim S.U., Seo D.C. *et al.*: Effect of inorganic and organic germanium treatments on the growth of lettuce (*Lactuca sativa*). – *J. Korean Soc. Appl. Bi.* **52**: 389-396, 2009.

Díaz-Vivancos P., Clemente-Moreno M.J., Rubio M. *et al.*: Alteration in the chloroplastic metabolism leads to ROS accumulation in pea plants in response to plum pox virus. – *J. Exp. Bot.* **59**: 2147-2160, 2008.

Diao M., Ma L., Wang J.W.: Selenium promotes the growth and photosynthesis of tomato seedlings under salt stress by enhancing chloroplast antioxidant defense system. – *J. Plant Growth Regul.* **33**: 671-682, 2014.

Garg N., Manchanda G.: ROS generation in plants: boon or bane? – *Plant Biosyst.* **143**: 81-96, 2009.

Genty B., Briantais J.M., Baker N.R.: The relationship between the quantum yield of photosynthetic electron transport and quenching of chlorophyll fluorescence. – *Biochim. Biophys. Acta* **990**: 87-92, 1989.

Gill S.S., Tuteja N.: Reactive oxygen species and antioxidant machinery in abiotic stress tolerance in crop plants. – *Plant Physiol. Bioch.* **48**: 909-930, 2010.

Goodman S.: Therapeutic effects of organic germanium. – *Med. Hypotheses* **26**: 207-215, 1988.

Halperin S.J., Barzilay A., Carson M. *et al.*: Germanium accumulation and toxicity in barley. – *J. Plant Nutr.* **18**: 1417-1426, 1995.

Han M.J., Kim S.U., Seo D.C. *et al.*: Uptake properties of germanium to vegetable plants and its effect on seed germination and on early stage growth. – *Korean J. Environ. Agric.* **26**: 217-222, 2007.

Hasanuzzaman M., Fujita M.: Selenium pretreatment upregulates the antioxidant defense and methylglyoxal detoxification system and confers enhanced tolerance to drought stress in rapeseed seedlings. – *Biol. Trace Elem. Res.* **143**: 1758-1776, 2011.

Henriques F.S.: Leaf chlorophyll fluorescence: background and fundamentals for plant biologists. – *Bot. Rev.* **75**: 249-270, 2009.

Jahns P., Holzwarth A.R.: The role of the xanthophyll cycle and of lutein in photoprotection of photosystem II. – *Biochim. Biophys. Acta* **1817**: 182-193, 2012.

Kaplan B.J., Parish W.W., Andrus G.M. *et al.*: Germane facts about germanium sesquioxide: I. Chemistry and anticancer properties. – *J. Altern. Complement. Med.* **10**: 337-344, 2004.

Kitajima M., Butler W.L.: Quenching of chlorophyll fluorescence and primary photochemistry in chloroplasts by dibromothymoquinone. – *Biochim. Biophys. Acta* **376**: 105-115, 1975.

Kramer D.M., Johnson G., Kuirats O., Edwards G.E.: New fluxparameters for the determination of QA redox state and excitation fluxes. – *Photosynth. Res.* **79**: 209-218, 2004.

Lazár D.: The polyphasic chlorophyll *a* fluorescence rise measured under high intensity of exciting light. – *Funct. Plant Biol.* **33**: 9-30, 2006.

Lichtenthaler H.K.: Chlorophylls and carotenoids: pigments of photosynthetic biomembranes. – *Methods Enzymol.* **148**: 350-382, 1987.

Li L., Zhou Z., Liang J., Lv R.: *In vivo* evaluation of the high-irradiance effects on PSII activity in photosynthetic stems of *Hexinia polydichotoma*. – *Photosynthetica* **53**: 621-624, 2015.

Lim J.S., Seo D.C., Park W.Y. *et al.*: Effects of soil texture on germanium uptake and growth in rice plant by soil application with germanium. – *Korean J. Environ. Agric.* **27**: 245-252, 2008.

Liu Y., Hou L.Y., Li Q.M. *et al.*: The effects of exogenous antioxidant germanium (Ge) on seed germination and growth of *Lycium ruthenicum* Murr subjected to NaCl stress. – *Environ. Technol.* **37**: 909-919, 2016.

Matsumoto H., Syo S., Takahashi E.: Translocation and some forms of germanium in rice plants. – *Soil Sci. Plant Nutr.* **21**: 273-279, 1975.

McMahon M., Regan F., Hughes H.: The determination of total germanium in real food samples including Chinese herbal remedies using graphite furnace atomic absorption spectroscopy. – *Food Chem.* **97**: 411-417, 2006.

Meyer S., Saccardi-Adji K., Rizza F., Genty B.: Inhibition of photosynthesis by *Colletotrichum lindemuthianum* in bean leaves determined by chlorophyll fluorescence imaging. – *Plant Cell Environ.* **24**: 947-955, 2001.

Munakata T., Agai S., Kuwano K. *et al.*: Induction of interferon production by natural killer cells by organogermanium compound Ge-132. – *J. Interferon Res.* **7**: 69-76, 1987.

Nakano Y., Asada K.: Hydrogen peroxide is scavenged by ascorbate-specific peroxidase in spinach chloroplasts. – *Plant Cell Physiol.* **22**: 867-880, 1981.

Nickel R.S., Cunningham B.A.: Improved peroxidase assay method using leuco 2,3,6-trichloroindophenol and application to comparative measurements of peroxidase catalysis. – *Anal. Physiol.* **172**: 385-390, 1969.

Rao K.V.M., Sresty T.V.S.: Antioxidant parameters in the seedlings of pigeon pea (*Cajanus cajan* L. Millspaugh) in response to Zn and Ni stresses. – *Plant Sci.* **157**: 113-128, 2000.

Rosenberg E.: Germanium: environmental occurrence, importance and speciation. – *Rev. Environ. Sci. Bio.* **8**: 29-57, 2009.

Schansker G., Tóth S.Z., Strasser R.J.: Methylviologen and dibromothymoquinone treatments of pea leaves reveal the role of photosystem I in the Chl *a* fluorescence rise OJIP. – *Biochim. Biophys. Acta* **1706**: 250-261, 2005.

Schreiber U., Schliwa U., Bilger W.: Continuous recording of photochemical and non-photochemical chlorophyll fluorescence quenching with a new type of modulation fluorometer. – *Photosynth. Res.* **10**: 51-62, 1986.

Seo D.C., Cheon Y.S., Park S.K. *et al.*: [Applications of different types of germanium compounds on rice plant growth and its Ge uptake.] – *Korean J. Soil Sci. Fertil.* **43**: 166-173, 2010. [In Korean]

Sparks J.P., Chandra S., Derry L.A. *et al.*: Subcellular localization of silicon and germanium in grass root and leaf tissues by SIMS: evidence for differential and active transport. – *Biogeochemistry* **104**: 237-249, 2011.

Stepien P., Klobus G.: Antioxidant defense in the leaves of C3 and C4 plants under salinity stress. – *Physiol. Plantarum* **125**: 31-40, 2005.

Stirbet A., Govindjee: On the relation between the Kautsky effect (chlorophyll *a* fluorescence induction) and photosystem II: Basics and applications of the OJIP fluorescence transient. – *J. Photoch. Photobio. B* **104**: 236-257, 2011.

Strasser R.J.A., Srivastava A., Tsimilli-Michael M.: The fluorescence transient as a tool to characterize and screen photosynthetic samples. – In: Yunus M., Pathre U., Mohanty P. (ed.): *Probing Photosynthesis: Mechanisms, Regulation and Adaptation*. Pp. 445-483. Taylor and Francis, London 2000.

Takahashi S., Murata N.: How do environmental stresses accelerate photoinhibition? – *Trends Plant Sci.* **13**: 178-182, 2008.

Tang Z., Shi Y., Zhou J.P. *et al.*: Effects of an organogermanium compound on antioxidant function of vMDV-infected chickens. – *Chinese J. Vet. Sci.* **17**: 173-176, 1997. [In Chinese]

Tarakhovskaya E.R., Kang E.J., Kim K.Y., Garbary D.J.: Effect of GeO₂ on embryo development and photosynthesis in *Fucus vesiculosus* (Phaeophyceae). – *Algae* **27**: 125-134, 2012.

Yang M.K., Kim Y.G.: Protective role of germanium-132 against paraquat-induced oxidative stress in the livers of senescent accelerated mice. – *J. Toxicol. Environ. Health A* **58**: 289-297, 1999.

Wang Z.X., Chen L., Ai J. *et al.*: Photosynthesis and activity of photosystem II in response to drought stress in Amur Grape (*Vitis amurensis* Rupr.). – *Photosynthetica* **50**: 189-196, 2012.

Yu K.W., Murthy H.N., Jeong C.S. *et al.*: Organic germanium stimulated the growth of ginseng adventitious roots and ginsenoside production. – *Process. Biochem.* **40**: 2959-2961, 2005.

Zai X.M., Zhu S.N., Qin P. *et al.*: Effect of *Glomus mosseae* on chlorophyll content, chlorophyll fluorescence parameters, and chloroplast ultrastructure of beach plum (*Prunus maritima*) under NaCl stress. – *Photosynthetica* **50**: 323-328, 2012.

Zhang J.X., Kirkham M.B.: Antioxidant responses to drought in sunflower and sorghum seedlings. – *New Phytol.* **132**: 361-373, 1996.

Zhang M., Tang S.U., Huang X. *et al.*: Selenium uptake, dynamic changes in selenium content and its influence on photosynthesis and chlorophyll fluorescence in rice (*Oryza sativa* L.). – *Environ. Exp. Bot.* **107**: 39-45, 2014.